

1-1-2010

Markov random fields for abnormal behavior detection on highways

Son Lam Phung

University of Wollongong, phung@uow.edu.au

Philippe L. Bouttefroy

philippe@uow.edu.au

Abdesselam Bouzerdoum

University of Wollongong, bouzer@uow.edu.au

Azeddine Beghdadi

Follow this and additional works at: <https://ro.uow.edu.au/infopapers>



Part of the [Physical Sciences and Mathematics Commons](#)

Recommended Citation

Phung, Son Lam; Bouttefroy, Philippe L.; Bouzerdoum, Abdesselam; and Beghdadi, Azeddine: Markov random fields for abnormal behavior detection on highways 2010, 149-154.
<https://ro.uow.edu.au/infopapers/813>

Markov random fields for abnormal behavior detection on highways

Abstract

This paper introduces a new paradigm for abnormal behavior detection relying on the integration of contextual information in Markov random fields. Contrary to traditional methods, the proposed technique models the local density of object feature vector, therefore leading to simple and elegant criterion for behavior classification. We develop a Gaussian Markov random field mixture catering for multi-modal density and integrating the neighborhood behavior into a local estimate. The convergence of the random field is ensured by online learning through a stochastic clustering algorithm. The system is tested on an extensive dataset (over 2800 vehicles) for behavior modeling. The experimental results show that abnormal behavior for a pedestrian walking, running and cycling on the highway, is detected with 82% accuracy at the 10% false alarm rate, and the system has an overall accuracy of 86% on the test data.

Keywords

abnormal, behavior, markov, random, detection, fields, highways

Disciplines

Physical Sciences and Mathematics

Publication Details

Bouttefroy, P. L., Beghdadi, A., Bouzerdoum, A. & Phung, S. (2010). Markov random fields for abnormal behavior detection on highways. 2nd European Workshop on Visual Information Processing (pp. 149-154). USA: IEEE.

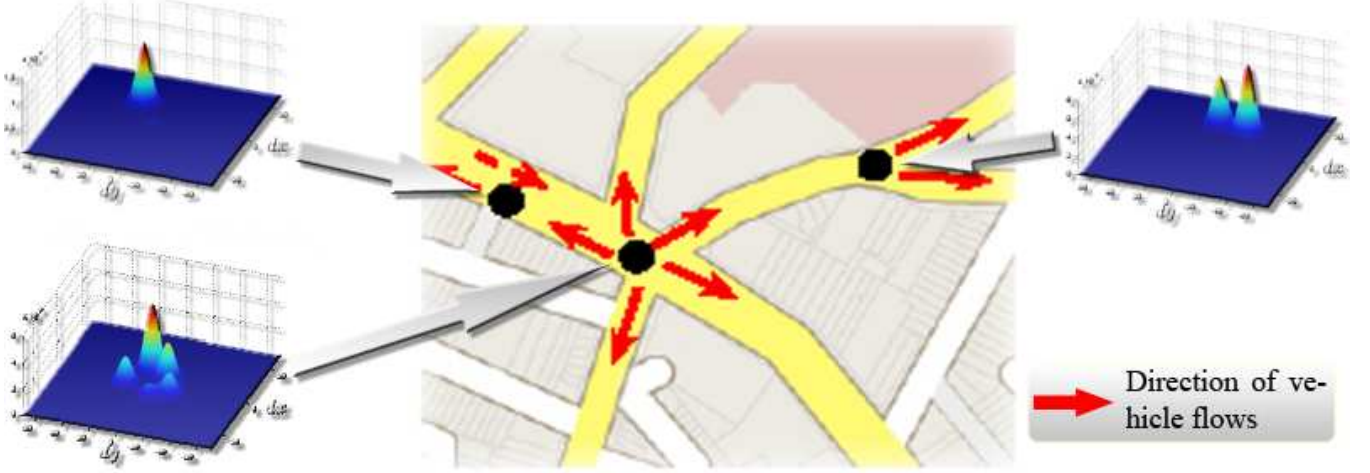


Fig. 1. Vehicle traffic scenario. The probability density function of vehicle displacements is represented for different sites. A global model would be cumbersome due to the complexity of implementation.

2.1. Markov Random Fields

Local modeling with a random field provides an accurate representation of vehicle displacements. Random fields are sets of random variables X_s arranged in graphs representing dependencies between nodes, called sites. A random field R is defined over a set of sites Ω such that $R = \{X_s : s \in \Omega\}$. In this paper, the sites are arranged in a 2-D lattice, representing the pixel locations in the image. A neighborhood η_s is a subset of Ω describing the spatial contiguity of site s with site n that satisfies $s \notin \eta_s$ and $s \in \eta_n \Leftrightarrow n \in \eta_s$. A clique $c \in \mathcal{C}$ is defined as a subset of a neighborhood where every site is adjacent to every other. R is a Markov random field if the probability of the realization r depends only on the neighborhood η_s , that is

$$P(r_s | r_{\Omega - \{s\}}) = P(r_s | r_{\eta_s}), \forall s \in \Omega. \quad (1)$$

The probability density of a MRF is given by the Gibbs probability density (Hammersley-Clifford theorem):

$$p(r) = \frac{1}{Z} \exp\left(-\frac{1}{T}U(r)\right), \quad (2)$$

where $Z = \int \exp(-U(r)/T)dr$ is a normalizing constant, T is the temperature and $U(r)$ is the energy function.

2.2. MRF Energy Function

Here, we consider the energy function to be composed of two potentials, a clique potential $V_c(r)$ and a spatial neighborhood potential $V_{\eta_s}(r)$, such that

$$U(r) = \sum_{c \in \mathcal{C}} V_c(r) + \sum_{s \in \Omega} V_{\eta_s}(r). \quad (3)$$

The potentials are modeled with a parametric density to maintain a compact representation of the field. The Gaussian function provides a practical representation of probability density with two parameters: the mean μ and the covariance Σ . Let θ_c represent the distribution parameters $\theta_c = \{\mu_c, \Sigma_c\}$. Here, the clique energy $V_c(r|\theta_c)$ is defined as the Mahalanobis distance

$$V_c(r|\theta_c) = \frac{1}{2}(r - \mu_c)^T \Sigma_c^{-1}(r - \mu_c). \quad (4)$$

Furthermore, the spatial energy $V_{\eta_s}(r|n)$ models the dependency of the site s on a neighboring site $n \in \eta_s$ as

$$V_{\eta_s}(r|n) = \frac{(s - n)^2}{2\sigma^2}, \quad (5)$$

where σ is a scaling parameter. The clique and spatial probabilities are subsequently defined as

$$P_c(r|\theta_c) = \exp(-V_c(r|\theta_c))/\lambda_c$$

and

$$P_{\eta_s}(r|n) = \exp(-V_{\eta_s}(r|n))/\lambda_n,$$

where λ_c and λ_n are normalizing constants. The aforementioned assumptions result in a Gaussian distribution over the MRF, leading to the so-called Gaussian Markov Random Field (GMRF) modeled with $p(r|\theta)$, the estimate of $p(r)$.

2.3. Gaussian Markov Random Field Mixture

The Gaussian Markov random field provides a unimodal estimate of the local behavior through the clique and spatial potentials. However, a multimodal estimate widens the scope of Markov random fields to cater for more intricate behavior

densities. For instance, the modeling of local displacement densities for the scenario presented in Fig. 1 requires such an estimate. For the problem of behavior modeling on highways, the challenge becomes more complex since the vehicle paths are not explicit (*e.g.* vehicle overtaking, stopping on the emergency lane, etc.). A mixture of K Gaussian random fields is therefore introduced as

$$p(r|\Theta) = \sum_{k=1}^K w(k)p(r|\theta_{c,k}), \quad (6)$$

where Θ is the set of parameters θ_k , *i.e.*, $\Theta = \{\theta_1, \dots, \theta_k\}$ and the $w(k)$'s are the respective weights of each component in the mixture. It is implicitly assumed here that the number of modes at a given site is smaller than or equal to K . The Gaussian Markov random field mixture (GMRFM) offers a convenient representation of the local density after training, and leads to an efficient and elegant solution to abnormal behavior detection, using a simple matching criterion.

3. VEHICLE BEHAVIOR MODELING

The behavior of vehicles is modeled with the GMRF estimate introduced in Eq. (6). Because of the difficulty of characterizing abnormal behavior, a practical approach is considered: (i) obtain an accurate estimate of normal behavior; (ii) reject each vehicle displacement which does not fit to the normal behavior. The rejection criterion sets the boundary between normal and abnormal behavior.

3.1. Learning Normal Behavior

The learning of normal behavior via the estimate $p(r|\Theta)$ is performed through the tuning of the set of parameters Θ . The update is performed online for each realization of the random field with the maximum-likelihood (ML) technique. Traditionally, the update of the MRF is performed site-wise by *integration*: each site s is visited and the values of the neighborhood η_s are integrated in the estimate. In this paper, we update the MRF by *diffusion* of information at site s onto the neighborhood η_s . The fact that $s \in \eta_n \Leftrightarrow n \in \eta_s$ for MRFs ensures the equivalence of the two methods in terms of convergence to the true random field equilibrium. The two methods are also equivalent in terms of computation for fully populated realizations.

However, when events are sparse, diffusion avoids exhaustive and inefficient update of the random field estimate: only the set of active sites Ω_{l_t} is required in order to perform the update of the MRF. An active site is defined as the site of activity of a vehicle, a pedestrian, or any object of interest, *i.e.* where the feature vector representing the object is located. Therefore, if each realization \mathbf{x}_j is independent, the MRF can be updated sequentially. This results in the following equivalence

for the update of the MRF:

$$p(r|\Theta) \Leftrightarrow \{p(\mathbf{x}_j|\Theta) : j \in \Omega_{l_t}\}. \quad (7)$$

Traditionally, the ML estimator is used to determine the optimal value k^* for the parameter index as $k^* = \operatorname{argmax}_k [p(r_t|\Theta_t)]$ at each time step t . We use here a stochastic clustering algorithm to find the optimal k^* based on the clique probability for a given realization \mathbf{x}_j . It was shown by Bouzerdoum that a stochastic correction $\epsilon_{k,n} \sim \mathcal{N}(\cdot, 0, \sigma^2)$ improves the convergence of the clustering algorithm [4]. For an active site $s \in \Omega_{l_t}$, the stochastic clustering approach seeks the ML in the GMRFM at each site $n \in \eta_s$. Then, the set of parameters Θ_t and the set of weights are updated with a recursive filter. Algorithm 1 describes the procedure.

Algorithm 1 GMRFM learning

- 1: $y_{k,n} = P_c(\mathbf{x}_j|\theta_{k,n}) + \epsilon_{k,n}$,
 - 2: $k^* = \operatorname{argmax}_k (y_{k,n})$.
 - 3: $\alpha_n = \lambda P_c(\mathbf{x}_j|\theta_{k^*,n}) P_{\eta_s}(\mathbf{x}_j|n)$.
 - 4: $w_n(k) \leftarrow w_n(k) + P_{\eta_s}(\mathbf{x}_j|n)$,
 - 5: $\boldsymbol{\mu}_{k^*,n} \leftarrow (1 - \alpha_n) \boldsymbol{\mu}_{k^*,n} + \alpha_n \mathbf{x}_j$,
 - 6: $\boldsymbol{\Sigma}_{k^*,n} \leftarrow (1 - \alpha_n) \boldsymbol{\Sigma}_{k^*,n} + \alpha_n (\mathbf{x}_j - \boldsymbol{\mu}_{k^*,n})^T (\mathbf{x}_j - \boldsymbol{\mu}_{k^*,n})$,
 - 7: Normalize the set of weights $\{w_k\}_{k=1}^K$.
-

3.2. Simulated Annealing

The temperature T in Eq. (2) performs simulated annealing, a technique used to increase the convergence of slow processes. The training of the GMRFM requires a large number of field realizations that are not available when modeling behavior. Furthermore, it should be noted that each site of the MRF does not receive an equal amount of information. For instance, sites of high traffic receive more information than the ones with low traffic. Consequently, the simulated annealing should be local rather than global (as it is with the variable T). We integrate the simulated annealing into the stochastic clustering process through the variance σ . A gradual decrease in the value provides a rough convergence during the learning stage while a finer convergence is achieved as the variance is reduced. This cooling schedule is performed by a counter $c_{k^*,n}$ incremented with the spatial probability $P_{\eta_s}(\mathbf{x}_j|n)$ at each visit of site s

$$c_{k^*,n} \leftarrow c_{k^*,n} + P_{\eta_s}(\mathbf{x}_j|n), \quad (8)$$

and the standard deviation of the shaking process is updated as follows:

$$\sigma_{k,n} = \sigma_0 / c_{k^*,n}. \quad (9)$$

Table 1. Summary of Videos for Normal Behavior

Video Sequence	Duration	No. of Vehicles
Video_001	199s	74
Video_002	360s	115
Video_003	480s	252
Video_004	367s	132
Video_005	140s	33
Video_006	312s	83
Video_007	302s	84
Video_008	310s	89
Video_009	80s	42
Video_010	495s	503
Video_011	297s	286
Video_012	358s	183
Video_013	377s	188
Video_014	278s	264
Video_015	269s	267

3.3. Abnormal Behavior Detection

The complexity of abnormal behavior detection is dramatically reduced by the local approach adopted. In most cases, normal and abnormal behavior of objects cannot be detected from the global trajectory. For instance, in [2] we showed that drunk driving was better detected with a local model since DUI was characterized by the variance of the vehicle trajectory that is smoothed out when learning with a global approach. Abnormal behavior is therefore elegantly detected with the local modeling offered by the GMRFM. The ML estimator introduced above directly provides the component of the mixture with the best match to the feature vector \mathbf{x} representing the object behavior. We use a matching criterion in the clique probability to classify the behavior as normal/abnormal as follows:

$$\begin{cases} V_c(\mathbf{x}|\boldsymbol{\theta}) \leq \lambda & \rightarrow \text{"normal"}, \\ V_c(\mathbf{x}|\boldsymbol{\theta}) > \lambda & \rightarrow \text{"abnormal"}, \end{cases} \quad (10)$$

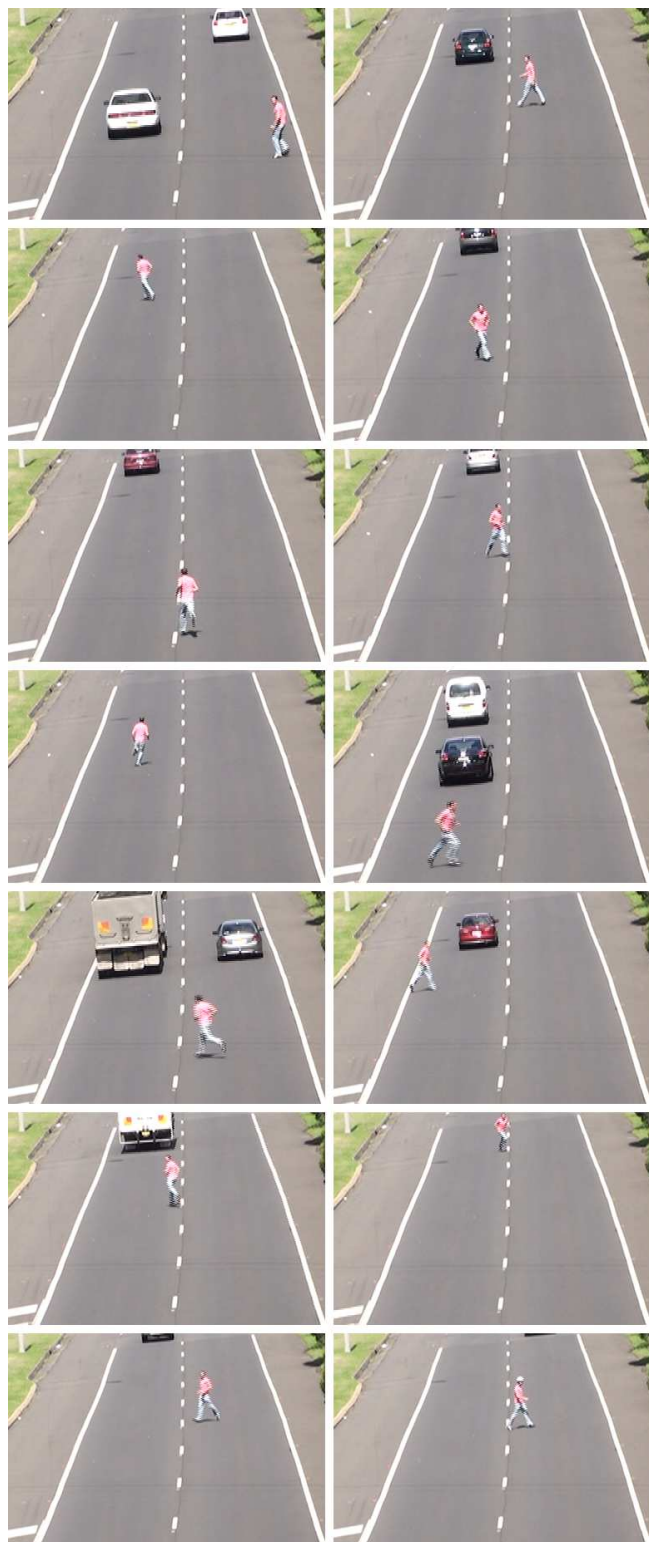
where $V_c(\mathbf{x}|\boldsymbol{\theta})$ represents the Mahalanobis distance.

4. EXPERIMENTAL SETUP AND RESULTS

This section is dedicated to the evaluation of the abnormal behavior detection with GMRFM on traffic monitoring video sequences. The vehicle traffic dataset and the experimental setup are described in Subsection 4.1. The performance of the algorithm is evaluated in Subsection 4.2.

4.1. Dataset and Experimental Setup

The proposed algorithm is tested on a traffic surveillance dataset including over 2800 vehicles. The dataset encompasses a large range of video footage with various settings (*e.g.*, height of the camera, angle of view, vanishing point

**Fig. 2.** Examples of abnormal behavior on highways.

position, etc.). The Projective Kalman filter, proposed recently by Bouttefroy *et al.* [3], is implemented for extracting

the object trajectories; it reduces the error in trajectory estimation by integrating the camera calibration settings into the Kalman filter equations. The trajectories are learnt for each video sequence individually since the settings vary from one video to another. The trajectory-based feature vector is composed of the position (x, y) and the vector flow (dx, dy) of the vehicle, *i.e.* $\mathbf{x} = [x, y, dx, dy]$. Due to the rarity of abnormal behavior, the 15 videos presented in Table 1 contain only normal behavior, which are used to train and test the system. In addition to this data, a video (Video_016) containing both normal and abnormal behaviors is tested. Sample frames from Video_016 sequence, representing abnormal behaviors on a highway, are displayed in Fig. 2: abnormal behavior consists of a person walking or riding a bike on the highway. There are 20 recorded trajectories for abnormal behavior, while there are more than 300 vehicles representing normal behavior in the video sequence. Here, normal behavior is modeled and abnormal behavior is detected as defined in Eq. (10); that is, trajectories not fitting the learnt model are considered abnormal.

4.2. Performance Analysis

To evaluate the performance of the system, the value of the threshold λ must first be estimated. This parameter determines the false alarm rate and the correct detection rate of abnormal behavior: a high threshold encourages normal behavior (see Eq. (10)) but lowers the rate of correct detection; a low threshold acts inversely. We want to estimate the threshold λ so that on average a 10% false detection rate is allowed on the dataset. Because abnormal behavior is only available in Video_16, the threshold is assumed to achieve a constant false detection rate across the entire dataset. This is a reasonable assumption since the Mahalanobis distance scales the distance of a feature vector with the variance, yielding a constant value for behavior/abnormal behavior boundary. In a preliminary experiment, the training of the MRF with Video_016 showed that a threshold of $\lambda = 0.0344$ achieves a 10% false detection rate with a correct detection rate of about 82%, see Fig. 3.

The algorithm is first tested on a pool of 15 videos representing normal behavior. The training for the estimation of the correct detection rate follows a 5-fold cross validation process: four fifths of the trajectories are used for training and one fifth for testing. The five-fold cross-validation process ensures that all data have been used in training and test sets. The results are summarized in Table 2. The average correct detection rate is 86.2% for a threshold value $\lambda = 0.0344$. The variation in the tracking rate for each video is due to the errors introduced in the track extraction. Video_004 presents the lowest correct tracking rate. The weak performance of the system on this video is due to the speed variation of vehicles. Indeed, because Video_004 is a close view of the highway, the accuracy of the object position is reduced and the classi-

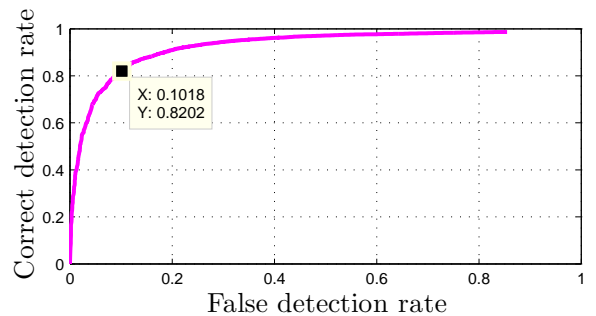


Fig. 3. ROC curve for the video sequence including abnormal behavior. The curve is explored by tuning the parameter λ . The value of 10% false detection rate gives a threshold value $\lambda = 0.0344$.

Table 2. Correct Detection Rate for the Video Dataset

Video Sequences	Correct Det.
Video_001	88.4%
Video_002	78.5%
Video_003	80.5%
Video_004	70.5%
Video_005	80.0%
Video_006	88.4%
Video_007	80.8%
Video_008	83.0%
Video_009	90.3%
Video_010	86.6%
Video_011	93.0%
Video_012	96.5%
Video_013	94.4%
Video_014	90.6%
Video_015	91.6%
Average	86.2%

fication is impaired. Normal behavior is characterized by a specific speed and direction of displacement of the vehicles. After sufficient training every object not matching these conditions is considered as having abnormal behavior.

Figure 4 displays the classification of each displacement in Video_016. It can be observed that the tracks of the vehicles (vertical) are considered normal (*blue*) in most cases. The false positive detections (normal behaviors considered abnormal) are due to tracking errors. Two cases can be differentiated: track loss and track uncertainty. In the first case, the tracker on the vehicle undergoes large variations in position when the track is lost. This results in displacements that do not fit the estimated density, and hence detected as abnormal. The second case occurs when there are smaller errors in the estimation of the object position due to uncertainty in tracking but the object is not lost. However, these variations are sufficient to misclassify the behavior as abnormal. On the other

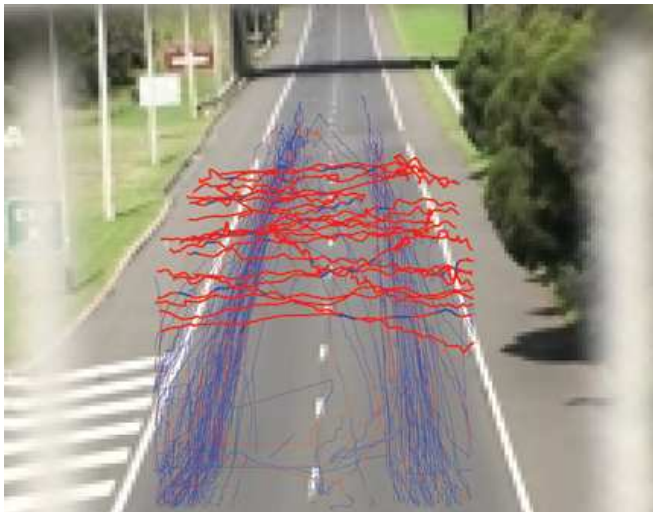


Fig. 4. Abnormal behavior detection rendering for a system trained and tested on real data. *Blue* represents the normal behavior; *red* the abnormal behavior.

hand, the person walking and cycling on the highway has an abnormal behavior. The system detects correctly abnormal behavior because the trajectories do not fulfill the norms of speed and direction.

5. CONCLUSION

This paper has presented a new framework for abnormal behavior detection. The Gaussian Markov random field mixture, modeling the local object behavior, integrates contextual information to carry out behavior modeling. The use of a clique and spatial neighborhood potential describing the energy function is proposed to account for the spatial dependencies between objects in a scenario. The training of the GMRFM is performed by a stochastic clustering algorithm.

The modeling of behaviors with the GMRFM enables an elegant detection of abnormal behavior since local densities are represented. A simple test applied to the Mahalanobis distance between the mode of the density and the feature vector provides efficient classification. The developed abnormal behavior detection was applied to video sequences of highway traffic. A video containing abnormal behavior is used as a benchmark to set up the behavior modeling. It results in a correct detection rate of 82% for a false detection rate of 10%. Moreover, the system achieves 86.2% correct detection rate on the entire dataset.

6. REFERENCES

[1] E. L. Andrade, S. Blunsden, and R. B. Fisher. Modelling crowd scenes for event detection. In *International Conference on Pattern Recognition*, volume 1, pages 175–178, 2006.

[2] P. L. M. Bouttefroy, A. Bouzerdoum, S. L. Phung, and A. Beghdadi. Abnormal behavior detection using a multi-modal stochastic learning approach. In *Proceedings of the International Conference on Intelligent Sensors, Sensor Networks and Information Processing*, pages 121–126, 2008.

[3] P. L. M. Bouttefroy, A. Bouzerdoum, S. L. Phung, and A. Beghdadi. Vehicle tracking by non-drifting mean-shift using projective kalman filter. In *Proceedings of the IEEE Conference on Intelligent Transportation Systems*, pages 61–66, 2008.

[4] A. Bouzerdoum. A stochastic competitive learning algorithm. In *Proceedings of the International Joint Conference on Neural Networks*, volume 2, pages 908–913, 2001.

[5] M. Dahmane and J. Meunier. Real-time video surveillance with self-organizing maps. In *Proceedings of the Canadian Conference on Computer and Robot Vision*, pages 136–143, 2005.

[6] T. V. Duong, H. H. Bui, D. Q. Phung, and S. A. Venkatesh. Activity recognition and abnormality detection with the switching hidden semi-markov model. In *Proceedings of the International Conference on Computer Vision and Pattern Recognition*, volume 1, pages 838–845, 2005.

[7] F. Jiang, Y. Wu, and A. K. Katsaggelos. Abnormal event detection from surveillance video by dynamic hierarchical clustering. In *IEEE International Conference on Image Processing*, volume 5, pages 145–148, 2007.

[8] D. Makris and T. Ellis. Path detection in video surveillance. *Image and Vision Computing*, 20:895–903, 2002.

[9] N. Vaswani and R. Chellappa. Non-stationary "shape activities". In *IEEE Conference on Decision and Control*, pages 1521–1528, 2005.

[10] Y. Wang, K. Huang, and T. Tan. Abnormal activity recognition in office based on r transform. In *IEEE International Conference on Image Processing*, volume 1, pages I – 341–I – 344, 2007.

[11] M. Weser, D. Westhoff, M. Huser, and Z. Jianwei. Multimodal people tracking and trajectory prediction based on learned generalized motion patterns. In *Proceedings of IEEE International Conference on Multisensor Fusion and Integration for Intelligent Systems*, pages 541–546, 2006.

[12] X. Wu, Y. Ou, H. Qian, and Y. Xu. A detection system for human abnormal behavior. In *International Conference on Intelligent Robots and Systems*, pages 1204–1208, 2005.

[13] T. Xiang and S. Gong. Video behavior profiling for anomaly detection. *IEEE Transactions on Pattern Analysis and Machine Intelligence*, 30(5):893–908, 2008.

[14] J. Yin, Q. Yang, and J. J. Pan. Sensor-based abnormal human-activity detection. *IEEE Transactions on Knowledge and Data Engineering*, 20(8):1082–1090, 2008.

[15] D. Zhang, D. Gatica-Perez, S. Bengio, and I. McCowan. Semi-supervised adapted hmms for unusual event detection. In *Proceedings of the International Conference on Computer Vision and Pattern Recognition*, volume 1, pages 611–618, 2005.